



# Mesoporous Strontium-Doped Phosphate-Based Sol-Gel Glasses for Biomedical Applications

Farzad Foroutan<sup>1</sup>, Benjamin Alexander Kyffin<sup>1</sup>, Isaac Abrahams<sup>2</sup>, Jonathan C. Knowles<sup>3,4,5,6</sup>, Elisa Sogne<sup>7</sup>, Andrea Falqui<sup>7</sup> and Daniela Carta<sup>1\*</sup>

<sup>1</sup> Department of Chemistry, University of Surrey, Guildford, United Kingdom, <sup>2</sup> School of Biological and Chemical Sciences, Materials Research Institute, Queen Mary University of London, London, United Kingdom, <sup>3</sup> Division of Biomaterials and Tissue Engineering, University College London, Eastman Dental Institute, London, United Kingdom, <sup>4</sup> The Discoveries Centre for Regenerative and Precision Medicine, London, United Kingdom, <sup>5</sup> Department of Nanobiomedical Science & BK21 PLUS NBM Global Research Centre for Regenerative Medicine, Dankook University, Cheonan-si, South Korea, <sup>6</sup> UCL Eastman-Korea Dental Medicine Innovation Centre, Dankook University, Cheonan-si, South Korea, <sup>7</sup> NABLA Lab, Biological and Environmental Sciences and Engineering (BESE) Division, King Abdullah University of Science and Technology (KAUST), Thuwal, Saudi Arabia

## OPEN ACCESS

### Edited by:

Tianyi Ma,  
University of Newcastle, Australia

### Reviewed by:

Xue Liu,  
Liaoning University, China  
Zhipeng Gu,  
Sun Yat-sen University, China  
Xin Du,  
University of Science and Technology  
Beijing, China

### \*Correspondence:

Daniela Carta  
d.carta@surrey.ac.uk

### Specialty section:

This article was submitted to  
Nanoscience,  
a section of the journal  
Frontiers in Chemistry

**Received:** 31 January 2020

**Accepted:** 16 March 2020

**Published:** 23 April 2020

### Citation:

Foroutan F, Kyffin BA, Abrahams I, Knowles JC, Sogne E, Falqui A and Carta D (2020) Mesoporous Strontium-Doped Phosphate-Based Sol-Gel Glasses for Biomedical Applications. *Front. Chem.* 8:249. doi: 10.3389/fchem.2020.00249

Mesoporous phosphate-based glasses have great potential as biomedical materials being able to simultaneously induce tissue regeneration and controlled release of therapeutic molecules. In the present study, a series of mesoporous phosphate-based glasses in the P<sub>2</sub>O<sub>5</sub>-CaO-Na<sub>2</sub>O system, doped with 1, 3, and 5 mol% of Sr<sup>2+</sup>, were prepared using the sol-gel method combined with supramolecular templating. A sample without strontium addition was prepared for comparison. The non-ionic triblock copolymer EO<sub>20</sub>PO<sub>70</sub>EO<sub>20</sub> (P123) was used as a templating agent. Scanning electron microscopy (SEM) images revealed that all synthesized glasses have an extended porous structure. This was confirmed by N<sub>2</sub> adsorption-desorption analysis at 77 K that shows a porosity typical of mesoporous materials. <sup>31</sup>P magic angle spinning nuclear magnetic resonance (<sup>31</sup>P MAS-NMR) and Fourier transform infrared (FTIR) spectroscopies have shown that the glasses are mainly formed by Q<sup>1</sup> and Q<sup>2</sup> phosphate groups. Degradation of the glasses in deionized water assessed over a 7-day period shows that phosphate, Ca<sup>2+</sup>, Na<sup>+</sup>, and Sr<sup>2+</sup> ions can be released in a controlled manner over time. In particular, a direct correlation between strontium content and degradation rate was observed. This study shows that Sr-doped mesoporous phosphate-based glasses have great potential in bone tissue regeneration as materials for controlled delivery of therapeutic ions.

**Keywords:** phosphate-based glasses, strontium-doped, tissue engineering, bioresorbable glasses, sol-gel

## INTRODUCTION

In recent years, mesoporous glasses have gained increased attention in the field of functional biomaterials (Baino et al., 2016). Their extended porosity, high surface areas and high pore volumes facilitate the interaction between the biomaterial and biological fluids. Moreover, therapeutic ions and molecules can be incorporated in the mesopores (pores size range 2–50 nm) with high loadings and released in a controlled manner (Wu and Chang, 2014). A significant amount of work has been performed on the synthesis of mesoporous silicate-based glasses mainly as drug delivery systems (Vallet-Regí et al., 2007; Yang et al., 2012) and for bone tissue regeneration applications (Zhang et al., 2016). However, only one very recent work has been presented on undoped

mesoporous phosphate-based glasses (Foroutan et al., 2020), for which the synthesis has been considered to be “a significantly challenging area for future efforts” in a recent review on sol-gel based materials for biomedical applications (Owens et al., 2016). In contrast to silicate-based glasses, phosphate-based glasses (PGs) have the particular property of being bioresorbable (Abou Neel et al., 2011). When in contact with body fluids, they slowly dissolve in the physiological environment and they are eventually totally replaced by regenerated tissue. Thanks to their complete solubility, PGs can be used as safe degradable temporary implants, avoiding the necessity of a second operation for their surgical removal (Knowles, 2003). As ions released from these glasses already exist in the body, problems related to toxicity and inflammatory reactions are avoided (Foroutan et al., 2015). However, silicate-based glasses have a poor solubility and typically they take several years to dissolve in a physiological environment (Fragogeorgi et al., 2019). Therefore, they cannot be used as temporary implants and their long-term effects in the body are still unknown. In addition, PGs offer advantages over polymer-based bioresorbable systems, as they do not leave any crystalline products upon dissolution. Release of crystalline fragments with heterogeneous chain-lengths during degradation of bioresorbable polymers has been reported to cause inflammatory reactions (Cheung et al., 2007; Sabir et al., 2009). Given their bioresorbability, PGs can be used as controlled local delivery systems of therapeutic species (e.g., antimicrobial ions/growth factors) that can be released in a controlled manner as the implant degrades. Controlled delivery avoids the need for oral administration and injection, improving the quality of life of patients (Wanakule and Roy, 2012; Wilczewska et al., 2012). The introduction of mesoporosity into PGs is expected to enhance the potential applications of these materials as controlled drug delivery systems, as the majority of ions/drugs used in clinical practice can easily be hosted in the mesopores (Vallet-Regí et al., 2007; Martínez-Carmona et al., 2018).

The conventional method to prepare PGs is the high temperature melt quenching technique (MQ), which involves heating the oxide precursors to temperatures in excess of 1,000°C (Ahmed et al., 2006; Al Qaysi et al., 2015). However, this method cannot be used for the production of porous PGs. Moreover, MQ often leads to non-homogeneous, bulk glasses that cannot be used for hosting temperature sensitive molecules. Recent studies have shown that PGs can be synthesized via the sol-gel method (SG) at much lower processing temperatures (Carta et al., 2005, 2007; Pickup et al., 2007; Foroutan et al., 2014). The sol-gel method is a wet chemical bottom-up technique based on the hydrolysis and polycondensation of alkoxide precursors in solution (Pickup et al., 2007; Owens et al., 2016). The use of precursors in solution allows the production of highly homogeneous glasses with controlled morphology (monoliths, porous foams, fibers, spheres, and thin films) (Carta et al., 2007; Lee et al., 2013). Additionally, by using the SG method, surfactant molecules can be easily added into the precursor solutions. Therefore, the SG process is ideal for the synthesis of mesoporous systems.

The surfactants spontaneously self-assemble in specific-shaped micelles at the critical micellar concentration, the shape and size depending on the specific surfactant used (Izquierdo-barba and Vallet-Regí, 2015). After removal of the surfactant

via calcination, pores having the sizes of the micelles are left in the inorganic material. The morphology of pores can be tailored thanks to the easily controlled solution-based chemistry.

In this study, mesoporous glasses in the  $P_2O_5$ -CaO- $Na_2O$  system doped with 1, 3, and 5 mol% of  $Sr^{2+}$  were successfully synthesized by the sol-gel method using the non-ionic block copolymer P123 as a templating agent. PGs in the  $P_2O_5$ -CaO- $Na_2O$  system have been shown to be effective materials for osteogenesis and controlled release of  $Ca^{2+}$  and  $Na^+$  ions as passive host materials for veterinary treatments (Abou Neel et al., 2011). There is great interest in doping these systems with functional ions. Several studies have been reported on  $P_2O_5$ -CaO- $Na_2O$  glasses doped with antibacterial ions such as  $Cu^{2+}$ ,  $Ag^+$ ,  $Zn^{2+}$ , and  $Ga^{3+}$  (Valappil et al., 2008; Abou Neel et al., 2011; Qaysi et al., 2016; Foroutan et al., 2019; Kyffin et al., 2019). During the last decade, the interest in the addition of  $Sr^{2+}$  to materials for bone regeneration has greatly increased due to the development of strontium ranelate as a promising drug for treating osteoporosis. Strontium has a unique effect on bone and can simultaneously promotes bone formation and inhibits bone resorption (Querido et al., 2016; Sriranganathan et al., 2016). Incorporation of strontium into silicate-based glasses has been shown to increase cell proliferation and normalized alkaline phosphatase activity in human osteosarcoma bone cells.  $Sr^{2+}$  also inhibited calcium phosphate resorption and reduced tartrate-resistant acid phosphatase activity, suggesting a dual action mechanism of released  $Sr^{2+}$  ions (Gentleman et al., 2010). Recent *in vivo* studies also demonstrated the effectiveness Sr-doped silicate-based glasses in promoting bone cells differentiation and proliferation in rabbits (Newman et al., 2014). In PGs, strontium has been incorporated only into MQ prepared systems (Abou Neel et al., 2009a; Al Qaysi et al., 2015; Sriranganathan et al., 2016). These studies confirmed the potential applications of Sr-doped PGs as effective vehicles to deliver  $Sr^{2+}$  to bone cells (Abou Neel et al., 2009a; Lakhkar et al., 2011). These glasses can also promote osteogenic differentiation of human mesenchymal stem cells that make them a great choice in various orthopedic, dental, and maxillofacial applications (Stefanic et al., 2018).

The majority of the  $P_2O_5$ -CaO- $Na_2O$  systems presented in the literature have been prepared via MQ; much less work has been done on analogous non-porous systems prepared via SG. In particular, no previous examples of mesoporous strontium-doped phosphate-based glasses have been presented in the literature. Therefore, here we presented for the first time a study on the sol-gel synthesis and characterization of strontium doped mesoporous phosphate-based glasses and the effect of strontium addition on dissolution properties.

## MATERIALS AND METHODS

### Synthesis

The following chemical precursors were used without further purification; n-butyl phosphate (1:1 molar ratio of mono  $OP(OH)_2(OBu^n)$  and di-butyl phosphate  $OP(OH)(OBu^n)_2$ , Alfa Aesar, 98%), calcium methoxyethoxide (Ca-methoxyethoxide, ABCR, 20% in methoxyethanol), sodium methoxide solution (NaOMe, Aldrich, 30 wt% in methanol), strontium acetate

(Sr-acetate, Aldrich, 97%), ethanol (EtOH, Fisher, 99%), and Pluronic (P123- $M_n = 5,800$ , Aldrich).

The target compositions in mol% of glasses were  $(P_2O_5)_{0.55}-(CaO)_{0.30}-(Na_2O)_{0.15-x}-(SrO)_x$ , with  $x = 1, 3, \text{ or } 5$ . In order to prepare the undoped glass, 1.7 g of n-butyl phosphate was added to 5 mL of EtOH in a dried vessel and left under stirring for 10 min. 3.5 g of Ca-methoxyethoxide and 0.5 g of NaOMe were then added dropwise into the mixture while stirring; the solution was kept under stirring for about 1 h. In order to prepare the Sr-doped glasses 0.04, 0.11, or 0.18 g of Sr-acetate were added to the mixture to prepare glasses containing  $x = 1, 3, \text{ or } 5$  mol% SrO, respectively; the quantity of NaOMe added was reduced accordingly. The mixtures were allowed to react for a further 10 min. Finally, a solution consisting of 3.0 g P123, 5 mL EtOH and 2.5 mL H<sub>2</sub>O was added to the mixtures and allowed to react for 10 min. The mixtures were poured into glass containers and allowed to gel at room temperature. Gelation occurred after about 5 min; gels were then aged for 1 day at room temperature. Then the temperature was increased from room temperature to 40°C and held for 1 day, to 60°C and held for 2 days, then to 80°C and held for 2 days, and finally to 120°C and held for 1 day before calcination at 300°C at a heating rate of 1°C·min<sup>-1</sup> to remove surfactant and solvents from the samples. The obtained glasses were ground at 10 Hz to form microparticles (MM301 milling

machine, Retsch GmbH, Hope, UK); microparticles in the size range of 106–200 μm were obtained using test sieves (Endecotts Ltd, London, UK). The sol-gel preparation of Sr-doped glasses is outlined in the flowchart in **Figure 1**. Glasses will be hereafter indicated MPG-und (undoped) and MPG-SrX (doped) where X = mol% SrO.

### Structural Characterization

X-ray powder diffraction (XRD, PANalytical X'Pert, Royston, UK) was performed on powdered samples in flat plate  $\theta/\theta$  geometry using Ni filtered Cu K $\alpha$  radiation. Data were collected using a PIXcel<sup>1D</sup> detector with a step size of 0.0525° over a 2 $\theta$  range of 10–90° and a time per step of 12 s.

SEM images reported in the main manuscript were performed with a JSM-7100F instrument (Jeol, Welwyn, UK) at an accelerating voltage of 10.0 kV and working distance of 10 mm. The samples were mounted onto aluminum stubs using carbon conductive tape. Pore sizes were measured using the Image-pro plus software (Media Cybernetics, USA). In order to determine the exact compositions of the prepared samples and compare them with the theoretical compositions energy dispersive X-ray spectroscopy (EDX, MagnaRay, ThermoFisher, Hemel Hempstead, UK) was performed using an SEM operating at 20.0 kV.

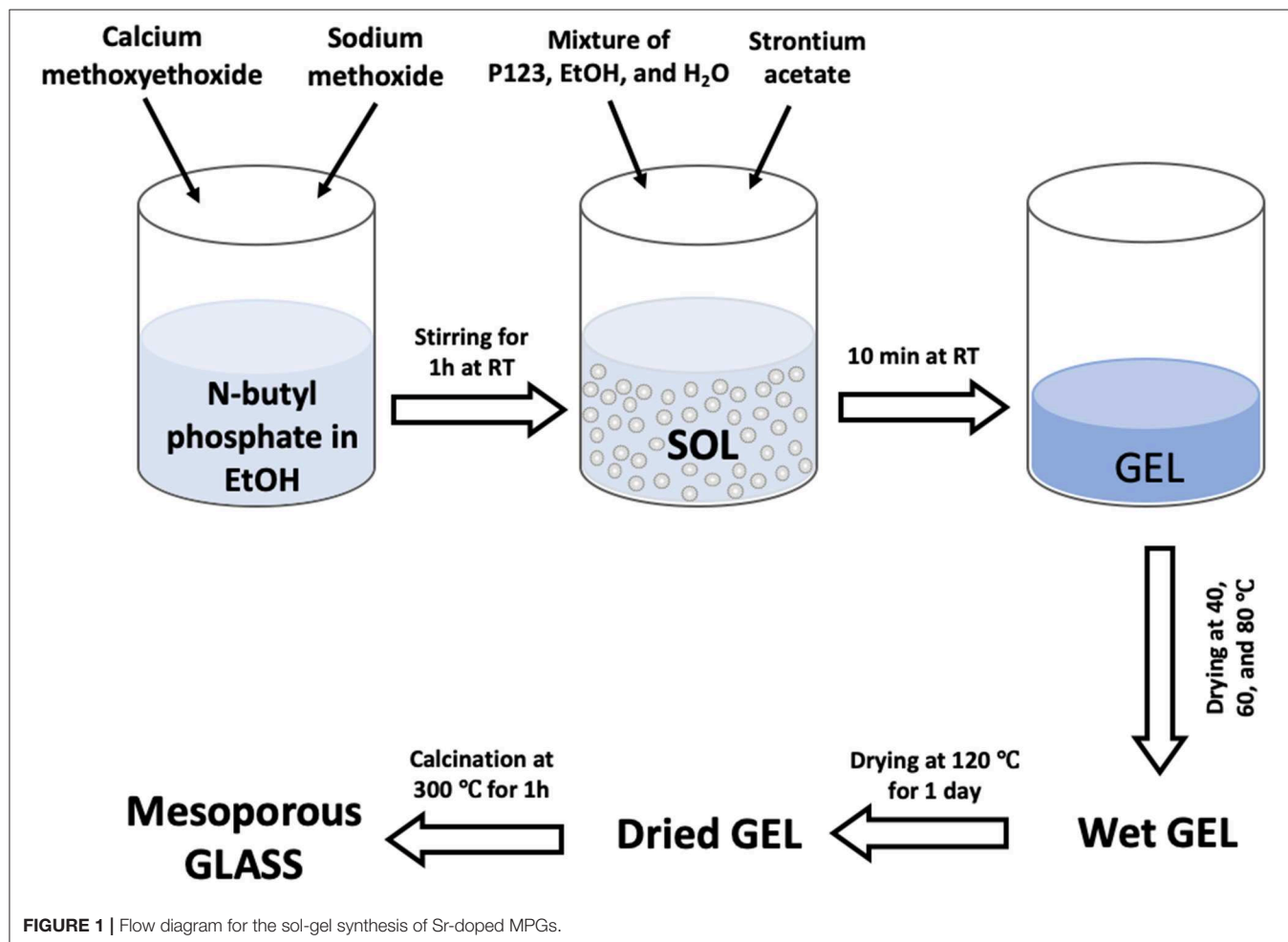


**FIGURE 1** | Flow diagram for the sol-gel synthesis of Sr-doped MPGs.

SEM images reported in the **Supplementary Information** were obtained by High-Resolution SEM (HRSEM) at very low acceleration voltage, using a FEI Magellan microscope equipped with a Field Emission Gun (FEG) electron source, imaging at high magnification the uncoated materials with an acceleration voltage of 1 kV, a probe current of 6.3 pA, an in-lens secondary electron detector and a monochromator (the FEI Wien filter called UC), the latter allowing for work with an energy spread of 0.15 eV FWHM, in order minimize any sample change induced by the electron beam, concomitantly getting a very surficial imaging with an ultimate lateral resolution of <1 nm.

Solid state  $^{31}\text{P}$  MAS-NMR spectra (AVANCE III, Bruker, Coventry, UK) were recorded at 161.87 MHz using direct excitation with a  $90^\circ$  pulse and 60 s recycle delay at ambient probe temperature ( $\sim 25^\circ\text{C}$ ). Between 20 and 88 scans were acquired in each case. Powder samples were loaded into 4.0 mm outer diameter zirconia rotors and spun at 12 kHz. Spectra were referenced to the resonance of the secondary reference ammonium dihydrogen phosphate ( $\text{NH}_4\text{H}_2\text{PO}_4$ ) at 0.9 ppm (relative to 85%  $\text{H}_3\text{PO}_4$  solution at 0 ppm). Spectra were fitted using the Dmfit software package (Massiot et al., 2002).

FTIR spectra for each sample were acquired using a FTIR-2000 instrument equipped with Timebase software (Perkin Elmer, Seer Green, UK) with an attenuated total reflectance accessory (Golden Gate, Specac, Orpington, UK). Samples were scanned at room temperature in absorbance mode in the range of  $600\text{--}1,500\text{ cm}^{-1}$ .

$\text{N}_2$  adsorption-desorption analysis was performed on a Gemini V, Micromeritics, Hertfordshire, UK; in particular, the specific surface area was assessed by using the Brunauer-Emmett-Teller (BET) method, and the pores size distribution was determined from the desorption branch of the isotherm through the Broekhoff-de Boer (BdB) method and the Barrett-Joyner-Halenda (BJH) method.

## Degradation Study

10 mg of powdered samples were immersed in 10 mL deionized water for 1, 3, 5, and 7 days ( $n = 3$ ) at  $37^\circ\text{C}$ . The resulting

suspensions for each time point were then centrifuged at 4,800 rpm for 10 min to separate the powder glasses from the solution. Phosphorus, calcium, sodium, and strontium in solution were subsequently measured by ICP-OES (720ES-Varian, Crawley, UK) calibrated across the predicted concentration range using standard premade solutions (ICP multi-element standard solution, VWR). Both samples and standards were diluted in a 1:1 ratio with 4%  $\text{HNO}_3$  (Honeywell, Fluka<sup>TM</sup>). A blank (2%  $\text{HNO}_3$ ) solution was used as a reference under standard operating conditions. Simulated body fluid (SBF) or phosphate buffered saline (PBS) as alternative media solutions were not used as they contain  $\text{Ca}^{2+}$ ,  $\text{Na}^+$  and phosphate anions that would have interfered with the quantification of the small amount of the same ions released from the glasses.

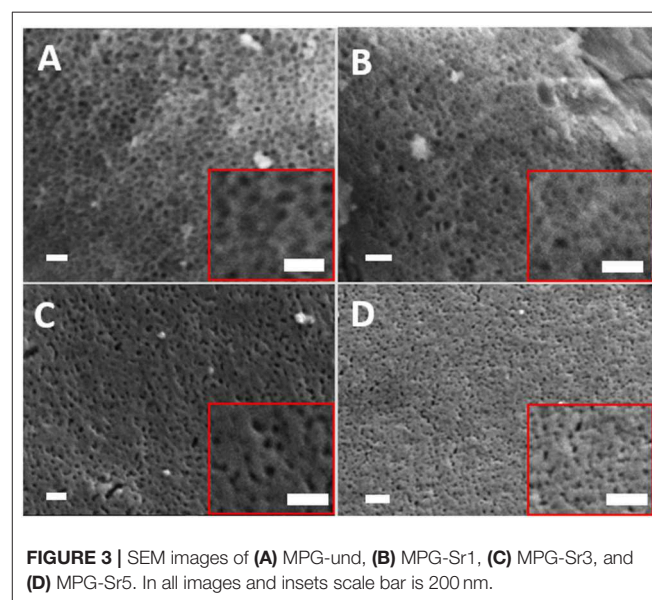
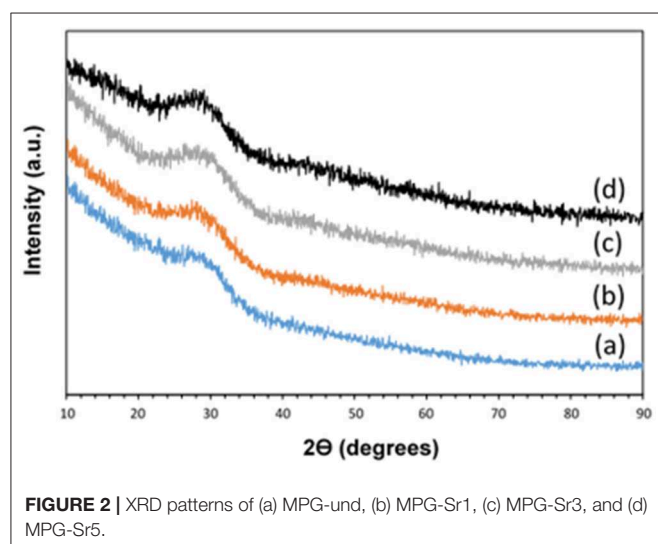
## RESULTS AND DISCUSSION

XRD was performed in order to assess glass formation and absence of crystallinity. The XRD patterns of all samples are reported in **Figure 2**. No Bragg peaks are present confirming the amorphous nature of the samples prepared. Only a broad halo centered at  $2\theta \sim 29^\circ$  can be observed, due to the phosphate glass network.

The composition of the glasses was determined via chemical analysis carried out using SEM equipped with an EDX detector.

**TABLE 1** | Compositions of MPGs measured by EDX (mol%).

Sample code	$\text{P}_2\text{O}_5$	CaO	$\text{Na}_2\text{O}$	SrO
MPG-und	$45.0 \pm 1.2$	$36.0 \pm 1.0$	$19.0 \pm 0.6$	–
MPG-Sr1	$45.3 \pm 1.4$	$35.7 \pm 0.9$	$17.9 \pm 0.5$	$1.1 \pm 0.2$
MPG-Sr3	$44.6 \pm 0.8$	$36.4 \pm 1.1$	$15.8 \pm 0.9$	$3.2 \pm 0.5$
MPG-Sr5	$45.1 \pm 0.7$	$36.1 \pm 0.6$	$13.7 \pm 0.5$	$5.3 \pm 0.3$



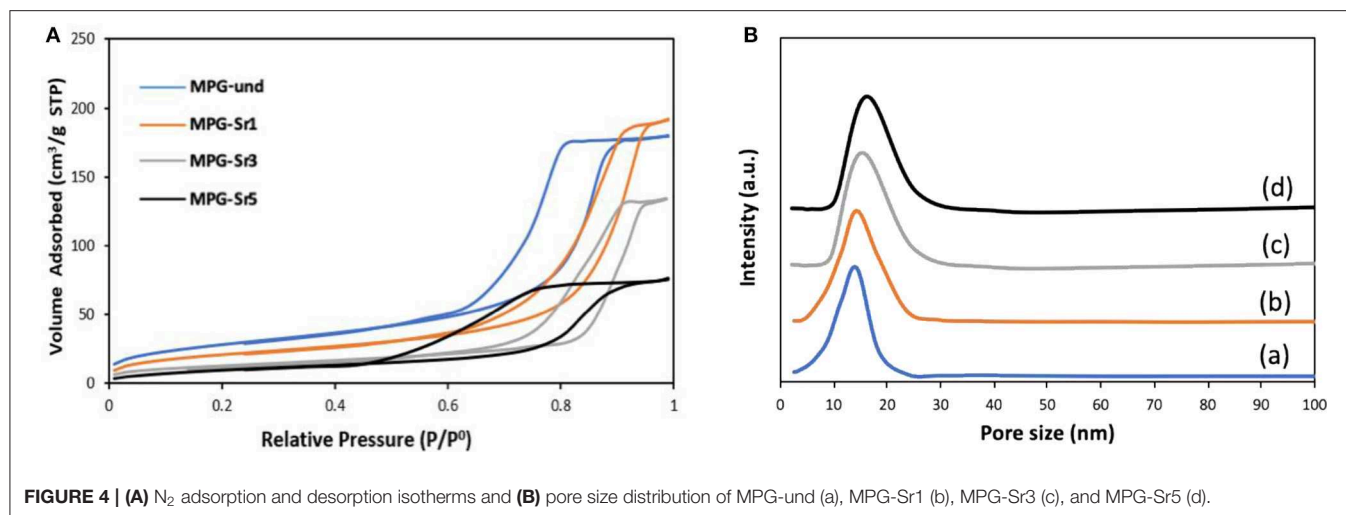


FIGURE 4 | (A) N<sub>2</sub> adsorption and desorption isotherms and (B) pore size distribution of MPG-und (a), MPG-Sr1 (b), MPG-Sr3 (c), and MPG-Sr5 (d).

TABLE 2 | Textural properties of MPGs.

Sample code	Surface area (m <sup>2</sup> ·g <sup>-1</sup> )	Pore size (nm)
MPG-und	123	11.8
MPG-Sr1	112	13.2
MPG-Sr3	94	15.1
MPG-Sr5	73	18.6

Sample compositions in terms of mol% are reported in Table 1; elemental compositions in terms of weight % along with a representative EDX spectra are reported in Table S1 and Figure S1, respectively.

The P<sub>2</sub>O<sub>5</sub> content showed a reduction of around 9–10 mol% from the theoretical values. Previous studies on MQ and SG phosphate-based glasses have shown that a P<sub>2</sub>O<sub>5</sub> content in the range 40–55 mol% and CaO content in the range 20–40 mol% have good bioactivity and biocompatibility (Carta et al., 2005; Abou Neel et al., 2009b; Al Qaysi et al., 2015).

The removal of the organic micelles of Pluronic (P123) by slow heating resulted in the formation of highly porous glasses. This is clearly shown in the SEM images reported in Figure 3. The mean pore sizes calculated from SEM images are 22, 21, 20, and 22 nm for MPG-und MPG-Sr1, MPG-Sr3, and MPG-Sr5, respectively. Histograms of pore size distribution obtained by statistical analysis of SEM images are reported in Figure S3.

Analysis of pore sizes was also performed by using N<sub>2</sub> adsorption-desorption analysis at 77 K. The N<sub>2</sub> adsorption-desorption isotherms and the pore size distribution curves for all the glasses are reported in Figures 4A,B, respectively. Surface areas and pore sizes are reported in Table 2.

The N<sub>2</sub> adsorption-desorption isotherms can be classified as type IV, characteristic of mesoporous solids. As the Sr<sup>2+</sup> content increases, the shape of the isotherm changes in particular for the glass with the highest strontium content. The surface area decreases with increasing Sr<sup>2+</sup> content from 123 m<sup>2</sup>·g<sup>-1</sup> (MPG-und) to 73 m<sup>2</sup>·g<sup>-1</sup> (MPG-Sr5). Even if the surface areas

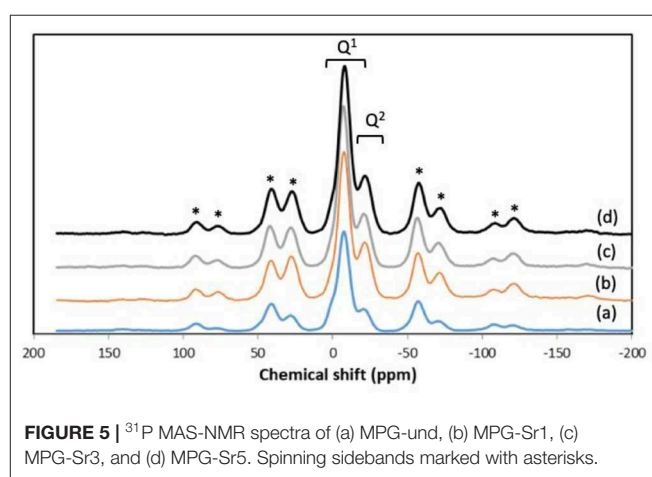


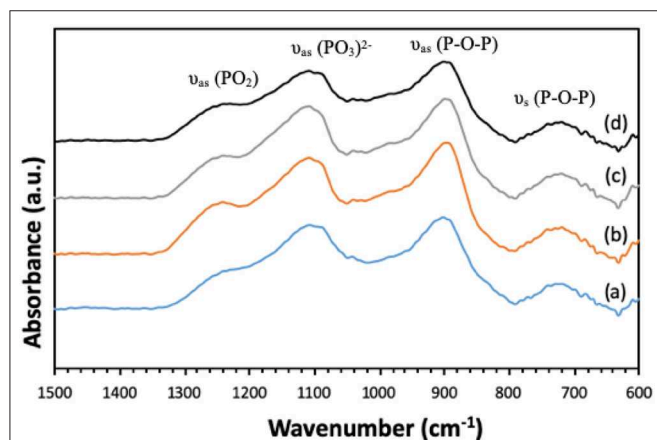
FIGURE 5 | <sup>31</sup>P MAS-NMR spectra of (a) MPG-und, (b) MPG-Sr1, (c) MPG-Sr3, and (d) MPG-Sr5. Spinning sidebands marked with asterisks.

are lower than typical mesoporous silicate-based glasses, this is a remarkable result giving that the calcium phosphate-based glasses are known to have a much weaker network structure than that of silicate-based systems. Pore size does not change significantly with strontium content and pore size distributions are all quite narrow. However, a slight increase in pore size is observed from 11.8 nm (MPG-und) to 18.6 nm (MPG-Sr5). It has been previously observed that higher dopant loading leads to higher pore sizes and lower surface areas in sol-gel zinc-doped silicate-based glasses (Courthéoux et al., 2008). This was ascribed to the modification of the network caused by the addition of the dopant.

In addition to textural properties, the structure of the phosphate network can also play a very important role, in particular in relation to dissolution properties. Therefore, we have investigated the structure of the phosphate network using <sup>31</sup>P MAS-NMR. This technique is a very powerful tool for the investigation of the connectivity of the phosphate units and the local environment around phosphorus. The <sup>31</sup>P MAS-NMR spectra of all samples are presented in Figure 5 and the

**TABLE 3** |  $^{31}\text{P}$  MAS-NMR spectral parameters (chemical shift,  $\delta_{\text{iso}}$ ) and relative intensity ( $I$  %).

Sample code	Q <sup>1</sup>		Q <sup>2</sup>	
	$\delta_{\text{iso}}$ (ppm)	$I$ % ( $\pm 1$ )	$\delta_{\text{iso}}$ (ppm)	$I$ % ( $\pm 1$ )
MPG-und	-6.2	68.3	-22.9	31.7
MPG-Sr1	-6.4	62.4	-23.0	37.6
MPG-Sr3	-6.5	61.9	-23.1	38.1
MPG-Sr5	-6.8	60.3	-23.6	39.7

**FIGURE 6** | FTIR spectra of (a) MPG-und, (b) MPG-Sr1, (c) MPG-Sr3, and (d) MPG-Sr5.

spectral parameters and assignments are reported in **Table 3**. Resonances are assigned to Q<sup>n</sup> phosphate species, where *n* represents the number of bridging oxygens between phosphate units. All spectra look very similar, with resonances in the range  $-6.2/-6.8$  ppm corresponding to Q<sup>1</sup> groups and  $-22.9/-23.6$  ppm corresponding to Q<sup>2</sup> groups (Foroutan et al., 2019). However, as the Sr content increases, the intensity of Q<sup>1</sup> groups decreases and the intensity of Q<sup>2</sup> groups increases.

Presence of Q<sup>1</sup> and Q<sup>2</sup> units in the phosphate chains was also confirmed by FTIR measurements. All FTIR spectra, reported in **Figure 6**, show similar bands, assigned on the basis of previous FTIR studies on phosphate-based glasses (Abou Neel et al., 2009a; Foroutan et al., 2019). The peak at  $730\text{ cm}^{-1}$  can be assigned to the symmetrical stretching  $\nu_s$  (P-O-P) mode, while the peak at  $900\text{ cm}^{-1}$  can be assigned to the asymmetrical stretching  $\nu_{\text{as}}$  (P-O-P) mode (Q<sup>2</sup> phosphate units). The peaks at  $1,100$  and  $1,235\text{ cm}^{-1}$  are also assigned to asymmetrical  $\nu_{\text{as}}$  (PO<sub>3</sub>)<sup>2-</sup> and  $\nu_{\text{as}}$  (PO<sub>2</sub>) modes that can be related to Q<sup>1</sup> and Q<sup>2</sup> phosphate units, respectively.

In addition to structural characterization, assessment of glass degradation, and quantification of ion delivery over time was performed. ICP-OES analysis was carried out to determine the release profiles of P, Ca, Na, and Sr following immersion of the glasses in deionized water up to 7 days (**Figure 7**).

The highest release of phosphate ions and Na<sup>+</sup> is observed for the Sr<sup>2+</sup>-free glass (MPG-und). Phosphate ions and Na<sup>+</sup> release

decrease with increasing Sr<sup>2+</sup> content, being the decrease more significant after the first 24 h.

These results suggest that the solubility of the glasses decreases by adding Sr<sup>2+</sup>; the addition of Sr<sup>2+</sup> results in the formation of a more cross-linked glass structure, with increased stability of the glass network and hence, decrease the leaching of ions from glass network. This is in agreement with previous results on Sr<sup>2+</sup> doped MQ glasses (Al Qaysi et al., 2015; Kargozar et al., 2019). Furthermore, the decrease in Na<sup>+</sup> content with increasing Sr<sup>2+</sup> amount can also be explained considering that Sr<sup>2+</sup> was added in place of Na<sup>+</sup> in the synthesis (**Table 1**). Therefore, as the Sr<sup>2+</sup> content is increased, the amount of Na<sup>+</sup> available to be released is decreasing.

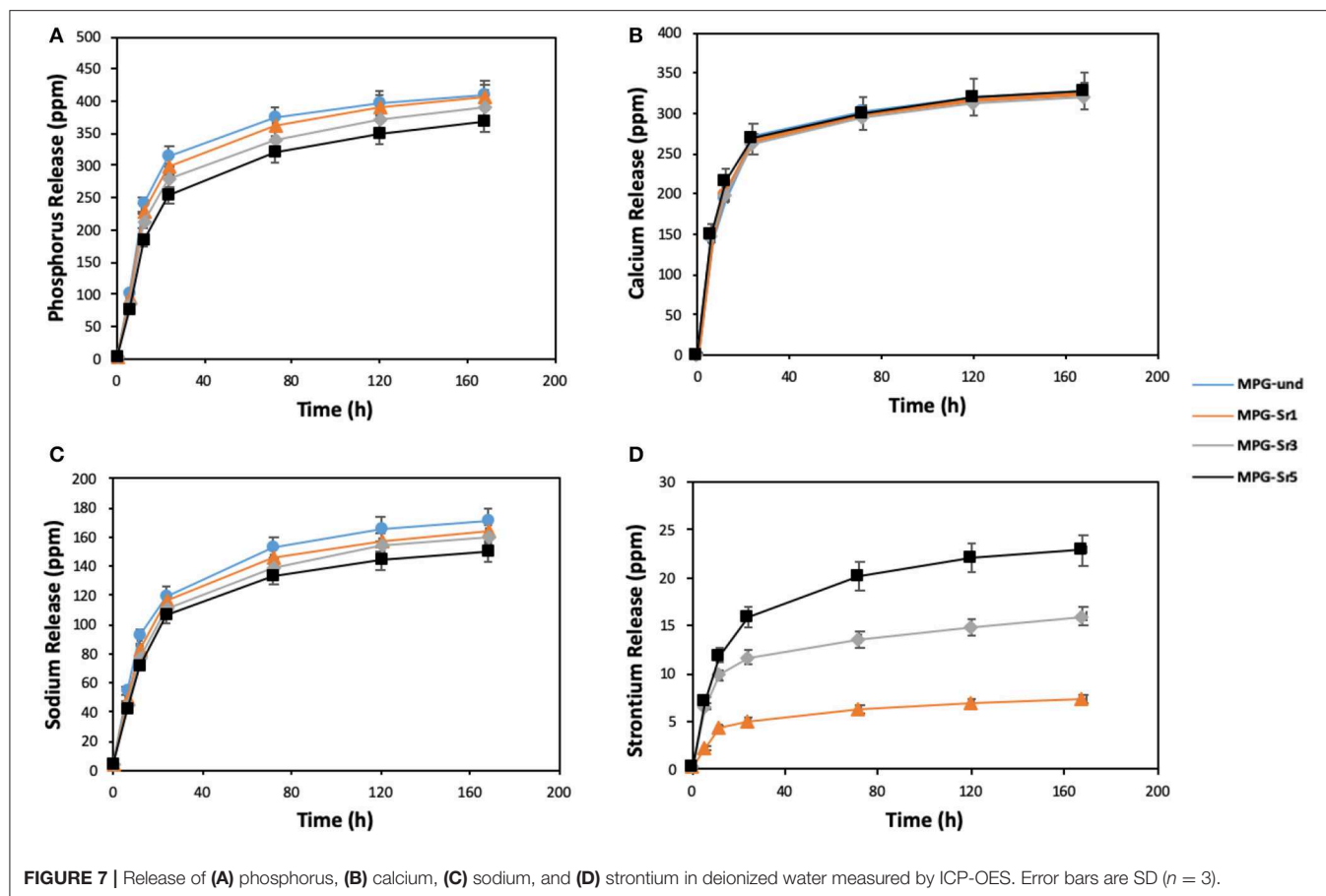
Interestingly, calcium release profiles do not change significantly with strontium loading. This suggests that Ca<sup>2+</sup> release is less affected by the decrease in glass solubility caused by Sr<sup>2+</sup> addition. Similar results were obtained using strontium-doped phosphate-based glasses prepared via MQ (Stefanic et al., 2018). Ca<sup>2+</sup> release was found to be independent of strontium loading; its release over time was very similar for systems containing 1, 5, and 10 mol% of SrO. Finally, Sr<sup>2+</sup> release increases with SrO content as expected, as higher amounts of Sr<sup>2+</sup> are available to be released in the glasses with higher Sr<sup>2+</sup> content. Sr<sup>2+</sup> ion release shows that is possible to control the amount of Sr<sup>2+</sup> released over time. The morphology of the glasses after immersion was also investigated. SEM images of the representative sample MPG-Sr3 after 1, 3, 5, and 7 days of immersion in deionized water are shown in **Figure S4**. The images show that high porosity is preserved even after 7 days of immersion.

To conclude, this study has shown that strontium-doped phosphate-based glasses with an extensive mesoporosity and high surface area can be prepared using the sol-gel technique. Moreover, it has been demonstrated that Sr<sup>2+</sup>, which is known to play an important role in bone tissue regeneration, can be delivered in a controlled way over time.

Given that MPG-und has very recently been shown to have enhanced bioactivity and biocompatibility compared to analogous non-porous PGs (Foroutan et al., 2020), strontium doped MPG are expected to show even higher enhancement in bone cell viability. The promising findings encourages further studies to evaluate the potential of these glasses for bone tissue regeneration and drug delivery.

## CONCLUSIONS

Mesoporous phosphate-based glasses in the P<sub>2</sub>O<sub>5</sub>-CaO-Na<sub>2</sub>O system doped with Sr<sup>2+</sup> = 1, 3, or 5 mol% were successfully prepared using the sol-gel method combined with the use of the surfactant block copolymer Pluronic 123. N<sub>2</sub> adsorption-desorption analysis at 77 K of all glasses shows isotherms that can be classified as type IV, characteristic of mesoporous solids. The surface area of the undoped P<sub>2</sub>O<sub>5</sub>-CaO-Na<sub>2</sub>O glass is  $123\text{ m}^2\cdot\text{g}^{-1}$ ; this value decreases upon addition of Sr<sup>2+</sup> being  $73\text{ m}^2\cdot\text{g}^{-1}$  for the sample doped with 5 mol% of Sr<sup>2+</sup>.  $^{31}\text{P}$  MAS-NMR and FTIR results revealed that the glass structure consists of mainly Q<sup>1</sup> and Q<sup>2</sup> phosphate units. Degradation of glasses



in deionized water shows that as the  $\text{Sr}^{2+}$  content increases, the glass degradation rate decreases. The results show that the prepared mesoporous Sr-doped phosphate-based glasses have potential as materials for controlled delivery of therapeutic ions, in particular for bone repair applications.

## DATA AVAILABILITY STATEMENT

The raw data supporting the conclusions of this article will be made available by the authors, without undue reservation.

## AUTHOR CONTRIBUTIONS

FF performed synthesis and characterization of MPG and PG. BK has helped with characterization (IR and SEM). IA has provided access to MAS NMR and assisted with  $^{31}\text{P}$  MAS NMR data analysis. JK has provided access to ICP and assisted with dissolution data analysis. ES and AF have performed SEM imaging at high resolution. DC has lead

the work and given expertise on data interpretation on all characterization techniques.

## FUNDING

This work was supported by EPSRC (grant EP/P033636/1) and Royal Society grant RSG\R1\180191.

## ACKNOWLEDGMENTS

The authors are grateful to Dr. David Jones for his help with the SEM/EDX and Dr. Graham Palmer for his help with ICP-OES measurements.

## SUPPLEMENTARY MATERIAL

The Supplementary Material for this article can be found online at: <https://www.frontiersin.org/articles/10.3389/fchem.2020.00249/full#supplementary-material>

## REFERENCES

- Abou Neel, E. A., Chrzanowski, W., Pickup, D. M., O'Dell, L. A., Mordan, J. N., Newport, R. J., et al. (2009a). Structure and properties of strontium-doped phosphate-based glasses. *J. R. Soc. Interface* 6, 435–446. doi: 10.1098/rsif.2008.0348
- Abou Neel, E. A., Pickup, D. M., Valappil, S. P., Newport, R. J., and Knowles, J. C. (2009b). Bioactive functional materials: a perspective on phosphate-based glasses. *J. Mater. Chem.* 19, 690–701. doi: 10.1039/B810675D
- Abou Neel, E. A., Salih, V., and Knowles, J. C. (2011). Phosphate-based glasses in comprehensive biomaterials. *J. Mater. Chem.* 13, 2395–2401. doi: 10.1016/B978-0-08-055294-1.00249-X

- Ahmed, I., Ready, D., Wilson, M., and Knowles, J. C. (2006). Antimicrobial effect of silver-doped phosphate-based glasses. *J. Biomed. Mater. Res. Part A* 79, 618–626. doi: 10.1002/jbma.a.30808
- Al Qaysi, M., Walters, N. J., Foroutan, F., Owens, G. J., Kim, H. W., Shah, R., et al. (2015). Strontium- and calcium-containing, titanium-stabilised phosphate-based glasses with prolonged degradation for orthopaedic tissue engineering. *J. Biomater. Appl.* 30, 300–310. doi: 10.1177/0885328215588898
- Baino, F., Fiorilli, S., and Vitale-Brovarone, C. (2016). Bioactive glass-based materials with hierarchical porosity for medical applications: review of recent advances. *Acta Biomater.* 42, 18–32. doi: 10.1016/j.actbio.2016.06.033
- Carta, D., Knowles, J. C., Smith, M. E., and Newport, R. J. (2007). Synthesis and structural characterization of  $P_2O_5$ -CaO- $Na_2O$  sol-gel materials. *J. Non. Cryst. Solids* 353, 1141–1149. doi: 10.1016/j.jnoncrysol.2006.12.093
- Carta, D., Pickup, D. M., Knowles, J. C., Smith, M. E., and Newport, R. J. (2005). Sol-gel synthesis of the  $P_2O_5$ -CaO- $Na_2O$ - $SiO_2$  system as a novel bioresorbable glass. *J. Mater. Chem.* 15, 2134–2140. doi: 10.1039/b414885a
- Cheung, H.-Y., Lau, K.-T., Lu, T.-P., and Hui, D. (2007). A critical review on polymer-based bio-engineered materials for scaffold development. *Compos. Part B Eng.* 38, 291–300. doi: 10.1016/j.compositesb.2006.06.014
- Courthéoux, L., Lao, J., Nedelec, J.-M., and Jallot, E. (2008). Controlled bioactivity in Zinc-doped sol-gel-derived binary bioactive glasses. *J. Phys. Chem. C* 112, 13663–13667. doi: 10.1021/jp8044498
- Foroutan, F., Carta, D., McGuire, J., Gupta, P., Nikolaou, A., Kyffin, B. A., et al. (2019). Antibacterial copper-doped calcium phosphate glasses for bone tissue regeneration. *ACS Biomater. Sci. Eng.* 5, 6054–6062. doi: 10.1021/acsbmaterials.9b01291
- Foroutan, F., de Leeuw, N. H., Martin, R. A., Palmer, G., Owens, G. J., Kim, H. W., et al. (2014). Novel sol-gel preparation of  $(P_2O_5)_{0.4}$ - $(CaO)_{0.25}$ - $(Na_2O)_x$ - $(TiO_2)_{0.35-x}$  bioresorbable glasses ( $X = 0.05, 0.1, \text{ and } 0.15$ ). *J. Sol. Gel Sci. Technol.* 73, 434–442. doi: 10.1007/s10971-014-3555-6
- Foroutan, F., Jokerst, J. V., Gambhir, S. S., Vermesh, O., Kim, H. W., and Knowles, J. C. (2015). Sol-gel synthesis and electrospinning of biodegradable  $(P_2O_5)_{55}$ - $(CaO)_{30}$ - $(Na_2O)_{15}$  glass nanospheres as a transient contrast agent for ultrasound stem cell imaging. *ACS Nano* 9, 1868–1877. doi: 10.1021/nn506789y
- Foroutan, F., Kyffin, B. A., Abrahams, I., Corrias, A., Gupta, P., Velliou, E. G., et al. (2020). Mesoporous phosphate-based glasses prepared via sol-gel. *ACS Biomater. Sci. Eng.* doi: 10.1021/acsbmaterials.9b01896
- Fragoorgi, E. A., Rouchota, M., Georgiou, M., Velez, M., Bouziotis, P., and Loudos, G. (2019). *In vivo* imaging techniques for bone tissue engineering. *J. Tissue Eng.* 10:2041731419854586. doi: 10.1177/2041731419854586
- Gentleman, E., Fredholm, Y. C., Jell, G., Lotfibakhshaiesh, N., O'Donnell, M. D., Hill, R. G., et al. (2010). The effects of strontium-substituted bioactive glasses on osteoblasts and osteoclasts *in vitro*. *Biomaterials* 31, 3949–3956. doi: 10.1016/j.biomaterials.2010.01.121
- Izquierdo-barba, L., and Vallet-Regí M. (2015). Mesoporous bioactive glasses: relevance of their porous structure compared to that of classical bioglasses. *Biomed. Glas.* 1, 140–150. doi: 10.1515/bglass-2015-0014
- Kargozar, S., Montazerian, M., Fiume, E., and Baino, F. (2019). Multiple and promising applications of strontium (Sr)-containing bioactive glasses in bone tissue engineering. *Front. Bioeng. Biotechnol.* 7:161. doi: 10.3389/fbioe.2019.00161
- Knowles, J. C. (2003). Phosphate based glasses for biomedical applications. *J. Mater. Chem.* 13, 2395–2401. doi: 10.1039/b307119g
- Kyffin, B. A., Foroutan, F., Raja, F. N. S., Martin, R. A., Pickup, D. M., Taylor, S. E., et al. (2019). Antibacterial silver-doped phosphate-based glasses prepared by coacervation. *J. Mater. Chem. B* 7, 7744–7755. doi: 10.1039/C9TB02195G
- Lakshkar, N., Abou Neel, E. A., Salih, V., and Knowles, J. C. (2011). Titanium and strontium-doped phosphate glasses as vehicles for strontium ion delivery to cells. *J. Biomater. Appl.* 25, 877–893. doi: 10.1177/0885328210362125
- Lee, I. H., Foroutan, F., Lakshkar, N. J., Gong, M. S., and Knowles, J. C. (2013). Sol-gel synthesis and structural characterization of  $P_2O_5$ -CaO- $Na_2O$  glasses. *Phys. Chem. Glass. J. Glass. Sci. Technol. Part B* 54, 115–120.
- Martínez-Carmona, M., Gun'ko, Y. K., and Vallet-Regí, M. (2018). Mesoporous silica materials as drug delivery: “The Nightmare” of bacterial infection. *Pharmaceutics* 10:279. doi: 10.3390/pharmaceutics10040279
- Massiot, D., Fayon, F., Capron, M., King, I., Le Calvé, S., Alonso, B., et al. (2002). Modelling one- and two-dimensional solid-state NMR spectra. *Magn. Reson. Chem.* 40, 70–76. doi: 10.1002/mrc.984
- Newman, S. D., Lotfibakhshaiesh, N., O'Donnell, M., Walboomers, X. F., Horwood, N., Jansen, J. A., et al. (2014). Enhanced osseous implant fixation with strontium-substituted bioactive glass coating. *Tissue Eng. Part A* 20, 1850–1857. doi: 10.1089/ten.tea.2013.0304
- Owens, G. J., Singh, R. K., Foroutan, F., Alqaysi, M., Han, C. M., Mahapatra, C., et al. (2016). Sol-gel based materials for biomedical applications. *Prog. Mater. Sci.* 77, 1–79. doi: 10.1016/j.pmatsci.2015.12.001
- Pickup, D. M., Guerry, P., Moss, R. M., Knowles, J. C., Smith, M. E., and Newport, R. J. (2007). New sol-gel synthesis of a  $(CaO)_{0.3}$ - $(Na_2O)_{0.2}$ - $(P_2O_5)_{0.5}$  bioresorbable glass and its structural characterisation. *J. Mater. Chem.* 17, 4777–4784. doi: 10.1039/b709955j
- Qaysi, M., Al Petrie, A., Shah, R., and Knowles, J. C. (2016). Degradation of zinc containing phosphate-based glass as a material for orthopedic tissue engineering. *J. Mater. Sci. Mater. Med.* 27:157. doi: 10.1007/s10856-016-5770-x
- Querido, W., Rossi, A. L., and Farina, M. (2016). The effects of strontium on bone mineral: a review on current knowledge and microanalytical approaches. *Micron* 80, 122–134. doi: 10.1016/j.micron.2015.10.006
- Sabir, M. I., Xu, X., and Li, L. (2009). A review on biodegradable polymeric materials for bone tissue engineering applications. *J. Mater. Sci.* 44, 5713–5724. doi: 10.1007/s10853-009-3770-7
- Sriranganathan, D., Kanwal, N., Hing, K. A., and Hill, R. G. (2016). Strontium substituted bioactive glasses for tissue engineered scaffolds: the importance of octacalcium phosphate. *J. Mater. Sci. Mater. Med.* 27:39. doi: 10.1007/s10856-015-5653-6
- Stefanic, M., Peroglio, M., Stanciu, A. M., Machado, G. C., Campbell, I., Kržmanc, M. M., et al. (2018). The influence of strontium release rate from bioactive phosphate glasses on osteogenic differentiation of human mesenchymal stem cells. *J. Eur. Ceram. Soc.* 38, 887–897. doi: 10.1016/j.jeurceramsoc.2017.08.005
- Valappil, S. P., Ready, D., Abou Neel, E. A., Pickup, D. M., Chrzanoski, W., O'Dell, L. A., et al. (2008). Antimicrobial gallium-doped phosphate-based glasses. *Adv. Funct. Mater.* 18, 732–741. doi: 10.1002/adfm.200700931
- Vallet-Regí, M., Balas, F., and Arcos, D. (2007). Mesoporous materials for drug delivery. *Angew. Chemie. Int. Ed.* 46, 7548–7558. doi: 10.1002/anie.200604488
- Wanakule, P., and Roy, K. (2012). “Drug delivery,” in *Tissue Engineering: Principles and Practices*. doi: 10.1201/b13978
- Wilczewska, A. Z., Niemirowicz, K., Markiewicz, K. H., and Car, H. (2012). Nanoparticles as drug delivery systems. *Pharmacol. Rep.* 64, 1020–1037. doi: 10.1016/S1734-1140(12)70901-5
- Wu, C., and Chang, J. (2014). Multifunctional mesoporous bioactive glasses for effective delivery of therapeutic ions and drug/growth factors. *J. Control. Release* 193, 282–295. doi: 10.1016/j.jconrel.2014.04.026
- Yang, P., Gai, S., and Lin, J. (2012). Functionalized mesoporous silica materials for controlled drug delivery. *Chem. Soc. Rev.* 41, 3679–3698. doi: 10.1039/c2cs15308d
- Zhang, X., Zeng, D., Li, N., Wen, J., Jiang, X., Liu, C., et al. (2016). Functionalized mesoporous bioactive glass scaffolds for enhanced bone tissue regeneration. *Sci. Rep.* 6:19361. doi: 10.1038/srep19361

**Conflict of Interest:** The authors declare that the research was conducted in the absence of any commercial or financial relationships that could be construed as a potential conflict of interest.

Copyright © 2020 Foroutan, Kyffin, Abrahams, Knowles, Sogne, Falqui and Carta. This is an open-access article distributed under the terms of the Creative Commons Attribution License (CC BY). The use, distribution or reproduction in other forums is permitted, provided the original author(s) and the copyright owner(s) are credited and that the original publication in this journal is cited, in accordance with accepted academic practice. No use, distribution or reproduction is permitted which does not comply with these terms.